



ECOLE  
**POLYTECHNIQUE**  
DE BRUXELLES

---

## Project ELEC-H415

---

### PROJECT REPORT : RAY-TRACING

*Student :*

TRILLET Antoine

*Professor :*

DE DONCKER Philippe

August 2022

# Contents

<b>1</b>	<b>Introduction</b>	<b>4</b>
<b>2</b>	<b>Theoretical foundations</b>	<b>5</b>
2.1	Antennas and received power . . . . .	5
2.2	Different types of ray considered . . . . .	6
2.2.1	Line-of-sight ray (LOS) . . . . .	6
2.2.2	Reflections on the walls . . . . .	7
2.2.3	Reflection on the ground . . . . .	7
2.2.4	Diffraction . . . . .	9
2.3	Received Power . . . . .	9
<b>3</b>	<b>Validation of results obtained by simulation</b>	<b>10</b>
<b>4</b>	<b>Results and Models</b>	<b>12</b>
4.1	Results for the full 2D map . . . . .	12
4.2	1D distribution from BS to eastern corner . . . . .	16
4.3	Model evaluation . . . . .	16
4.3.1	Path loss model . . . . .	17
4.3.2	Fading Variability . . . . .	18
4.3.3	Cell range . . . . .	18
4.4	Impulse responses . . . . .	20
4.4.1	Center of the square . . . . .	20

4.4.2	Eastern corner . . . . .	21
<b>5</b>	<b>Further discussion</b>	<b>23</b>
5.1	Propagation model for the rue de la Tête d'Or . . . . .	23
5.2	Reflectors and directivity manipulation . . . . .	24
5.2.1	Development of the directivity of the antenna + reflector . . . . .	25
5.2.2	Directing the beam towards the streets . . . . .	26
5.3	Optimisation using an interactive interface . . . . .	26
<b>6</b>	<b>Conclusion</b>	<b>28</b>
<b>A</b>	<b>TDL impulse responses</b>	<b>29</b>
<b>B</b>	<b>Interferences obtained for different values of d</b>	<b>30</b>

# Abstract

This project consists in the modelisation of the downlink channel from a 5G small cell base station(BS) toward a mobile user equipment(UE) on the grand place of Brussels. 2D heatmaps of the received power, SNR, delay spread and Rice factor at UE show the difficulty of 1 BS to communicate in the streets. A path loss model has been computed for the power distribution from the western to the eastern corner, with a path loss exponent  $n = 1.82$ , a fading variability of 5.2 and a cell range for 90 percent of connection of around 45m.

On top of the requirements for the project, a model for rue the la tête d'or has been done. Also the mathematical development for a metal reflector behind the antennas was made, with it we were able to predict where the interference would occur and how to manipulate the directivity to point the beam towards the streets. On top of the Ray-tracing and communication parameters proposed by the project description. The temperature is supposed to be 300K, the ground and buildings have a relative permittivity of 4, the bandwidth is 200MHz.

# 1. Introduction

5G cells will soon be deployed in urban areas to provide high data rate. These cells will be small enough to be placed at user height and urban furnitures. They will communicate at frequencies around 26GHz and use a bandwidth up to 200MHz. Of course, the connection probability in the street will highly depend on the geometry of the urban area in question and good modelisation of the power received around the area will help making good placement decision and avoid wasting antennas and energy. This is the main goal of this project that aims to make a simulation of the small cell channels using ray-tracing and image theory to simulate the propagation. The geometry is the Grand Place of Brussels and its surrounding streets and the red dot is the base station.

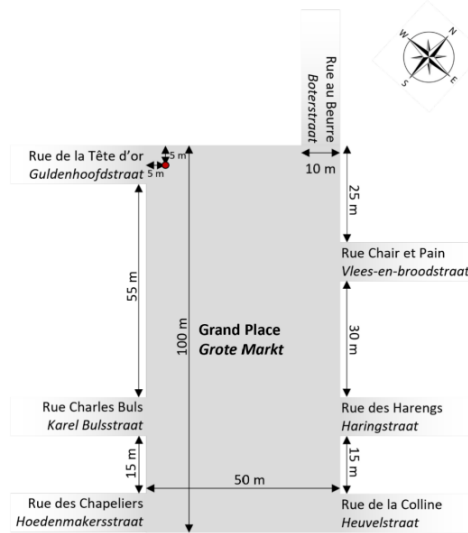


Figure 1: Approximate geometry of Grand Place / Grote Markt in Brussels

Figure 1.1: Approximate geometry of Grand Place

## 2. Theoretical foundations

The ray tracing algorithm evaluates the magnitude and phase of the electromagnetic waves(EM) seen at the UE, as well as the induced power. To do so it first determines all possible rays that reaches the UE from the base station(BS), straight, with reflections and/or refraction. Then it has to compute the voltage induced at the receiver by each ray, based on some assumptions, parameters and equations introduced in this section.

### 2.1 Antennas and received power

The antennas used in this project are vertical  $\lambda/2$  antennas working around 27Ghz. These are assumed to be vertical, not moving and at a height of 2 m. As these are at the same height most rays(all of them beside the ground reflections) will be perpendicular to the antennas leading to a fixed gain for the antennas in most cases, independant of the direction of propagation in the horizontal plane, worth:

$$G(\theta, \phi) = \frac{16}{3\pi} \sin^3 \theta \quad (2.1)$$

In free space, the Pointing vector gives the density of radiated power seen at the receiver antenna:

$$S = G_{TX}(\theta_{TX}, \phi_{TX}) \frac{P_{TX}}{4\pi d^2} = |\underline{E}|^2 / 2Z_0 \quad (2.2)$$

Where  $P_{TX} = 0.147W = 21.7dBm$  is the emitting power,  $d$  the length crossed by the EM wave and  $Z_0 = \sqrt{\frac{\mu_0}{\epsilon_0}} \approx Z_{air}$  the void characteristic impedance. To make things more compact, the notation  $EIRP = G_{TX}(\theta_{TX}, \phi_{TX})P_{TX}$  and  $EIRP_{max} = 0.25W$  will be used

from now on. Thus, the phasor of the electric field at UE in free space is given by:

$$\underline{E}(d) = \sqrt{60EIRP} \frac{e^{-j\beta d}}{d} \quad (2.3)$$

The voltage induced on the antenna depends on the effective height  $\vec{h}_e$  of the antenna, and the angle of incidence:

$$\underline{V}_{oc} = \vec{h}_e(\theta, \phi) \cdot \underline{\vec{E}}(\vec{r}) = h_e(\theta, \phi) \underline{E}(d) \cos(\theta - \pi/2) \quad (2.4)$$

$$\vec{h}_e(\theta) = -\frac{\lambda \cos\left(\frac{\pi}{2} \cos \theta\right)}{\pi \sin^2 \theta} \vec{1}_z \quad (2.5)$$

Thus,  $h_e = -\lambda/\pi$  for all rays in the horizontal plane.  $\theta$  being the angle between  $\vec{1}_z$  and the incident ray.

## 2.2 Different types of ray considered

The power at UE can be derived from the electrical field resulting from all multi-path components (MPC). Reflexion on the walls and ground, as well as the refractions will add a new component, possibly increasing the resulting power but also causing some fading as the phase of each ray can either be destructive or constructive. In this simulation we will only consider rays that have reflected once on the ground, maximum twice on the wall, refracted when there is no line of sight and the LOS ray.

### 2.2.1 Line-of-sight ray (LOS)

The line-of-sight ray is the ray that goes straight to the UE without interacting with the walls or ground. It is therefore the shortest ray and the one that carries the most power. Its electric field can be described by the formula in the free space case 2.3:

$$\underline{E}(d) = \sqrt{60EIRP} \frac{e^{-j\beta d}}{d} \quad (2.6)$$

In the LOS case, the ray is in the horizontal plane so that  $EIRP_{LOs} = EIRP_{max} = 0.25W$  and  $h_e = -\lambda/\pi$

### 2.2.2 Reflections on the walls

Once an EM wave reaches the edge between two regions of different permittivity, one part will be refracted into the material, out of which some will transmit through (this case is not considered in our simulation) and another part will be reflected by the wall with the same angle as the incident angle ( the ray stay in the horizontal plane as ). The electric field of such ray will be reduced by a factor,  $\Gamma_{\perp}$ , that can be shown to be:

$$\underline{E}_n = \Gamma_1 \Gamma_2 \dots \sqrt{60 EIRP} \frac{e^{-j\beta d_n}}{d_n} \quad (2.7)$$

$$\Gamma_{\perp} = \frac{\cos \theta_i - \sqrt{\epsilon_r} \sqrt{1 - \frac{1}{\epsilon_r} \sin^2 \theta_i}}{\cos \theta_i + \sqrt{\epsilon_r} \sqrt{1 - \frac{1}{\epsilon_r} \sin^2 \theta_i}} \quad (2.8)$$

Where  $\theta_i$  is the angle of incidence of the ray and  $\epsilon_r \approx 4$  is the relative permittivity between the walls(or ground) and the air( $\approx vacuum$ ).  $\Gamma_{\perp}$ , the perpendicular reflection coefficient, is used here because  $\vec{E}$  is polarized vertically in  $\vec{1}_z$ , perpendicularly to the horizontal plane, the plane of incidence.

### 2.2.3 Reflection on the ground

As shown on the figure 2.2, the reflection on the ground is not in the horizontal plane. This means that the reflection coefficient to use is  $\Gamma_{\parallel}$ , as  $\vec{E}$  is polarized in the in plane of incidence:

$$\Gamma_{\parallel} = \frac{\cos \theta_g - \frac{1}{\sqrt{\epsilon_r}} \sqrt{1 - \frac{1}{\epsilon_r} \sin^2 \theta_g}}{\cos \theta_g + \frac{1}{\sqrt{\epsilon_r}} \sqrt{1 - \frac{1}{\epsilon_r} \sin^2 \theta_g}} \quad (2.9)$$



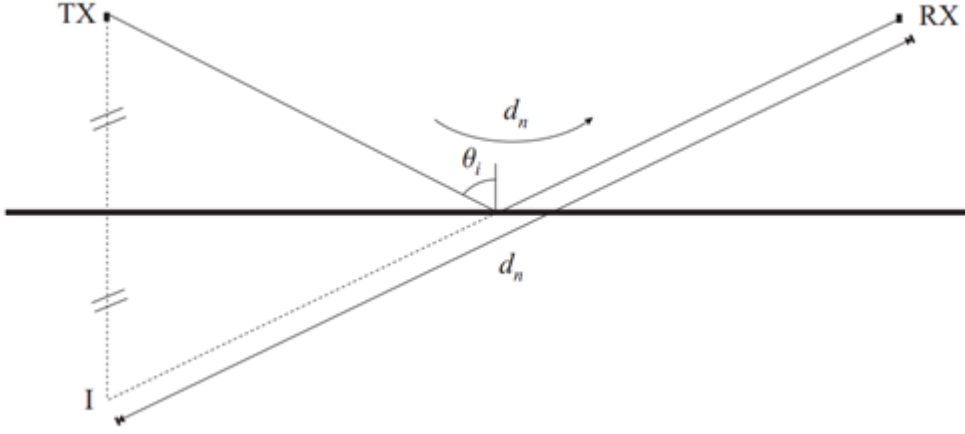


Figure 2.1: Image method for 1 reflection on a wall

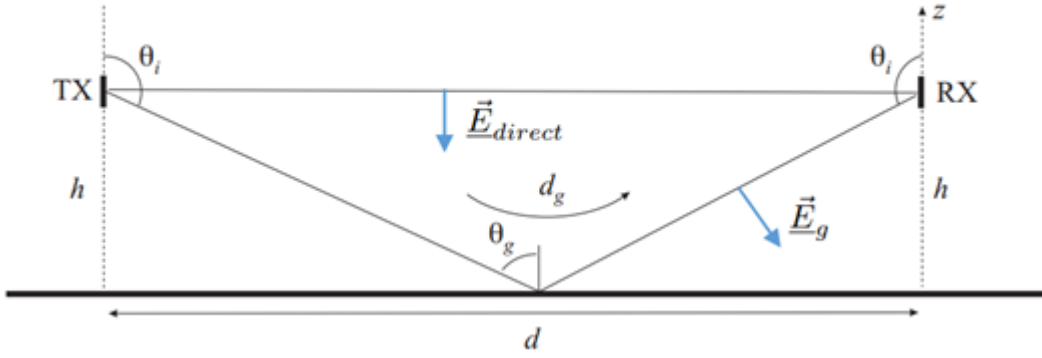


Figure 2.2: LOS and ground reflection geometry and rays

This also means that the angle between the antennas and the incoming or leaving ray is not  $90^\circ$  anymore.  $\theta_i = \theta_{TX} = \theta_{RX} = \pi - \theta_g$  which can be used to compute the  $EIRP(\theta_i)$ .

$$\theta_g = \arctan\left(\frac{d_g}{(2 * h)}\right) \quad (2.10)$$

$$d_g = \sqrt{(2 * h)^2 + (\Delta x)^2 + (\Delta y)^2} \quad (2.11)$$

### 2.2.4 Diffraction

Diffraction is taken into account when there is no line of sight but the EM wave meets an edge. The field behind the obstacle is due to the field radiated by the current induced in the obstacle. This is the knife edge model. The electric field at UE can be computed as for the LOS ray (equation 2.6) multiplied by a complex factor  $F(\nu)$ . An approximation of this factor is proposed by the ITU:

$$|F(\nu)|^2 [\text{dB}] \simeq -6,9 - 20 \log \left( \sqrt{(\nu - 0,1)^2 + 1} + \nu - 0,1 \right) \quad (2.12)$$

$$\text{Arg}F(\nu) = -\frac{\pi}{4} - \frac{\pi}{2}\nu^2 \quad (2.13)$$

$\nu$  is the Fresnel number that can be approximated by:

$$\nu = \sqrt{\frac{2}{\pi}} \beta \Delta r \quad (2.14)$$

Where  $\Delta r$  is the difference between the length of the direct path and the path going through the tip of the edge. The diffracted ray is supposed to follow the path through the tip, so that its propagation delay will be  $d_{tip}/c$ .

## 2.3 Received Power

The voltage induced at UE due to each MPC can be computed separately using equation 2.4. These then add up constructively or not, causing fading.

$$P_{RX} = \frac{\left| \sum_{n=1}^N \vec{h}_{e,n} \cdot \vec{E}_n \right|^2}{8R_a} = \frac{\left| \sum_{n=1}^N V_{oc,n} \right|^2}{8R_a} \quad (2.15)$$

### 3. Validation of results obtained by simulation

To validate that the code works as the model expects, the value of parameters and coefficients has been compared between the simulated version and hand-calculated one (using the equation shown in chapter 2) for 2 simple cases that consider all possible cases of ray. The emitting antenna is placed at the position (20,80), a wall is placed with edges at (60,90) and (60,50). The first reception antenna(n°1) is located at (40.5,60.5) to validate LOS, wall and ground-reflected. Another one(n°2) is at (80.5,80.5) to validate the diffracted rays.

The wall reflection is shown in blue on the 2D heatmap shown in fig 3.1, whether LOS and ground-reflected rays are in yellow and diffracted rays are in white ( $F(\nu)$  in the table below has been computed for the upper diffracted ray)

From this validation, it is reasonable to say that the algorithm gives the results expected from the equations provided. The small differences between hand-calculated and simulated figures are probably due to rounding errors.

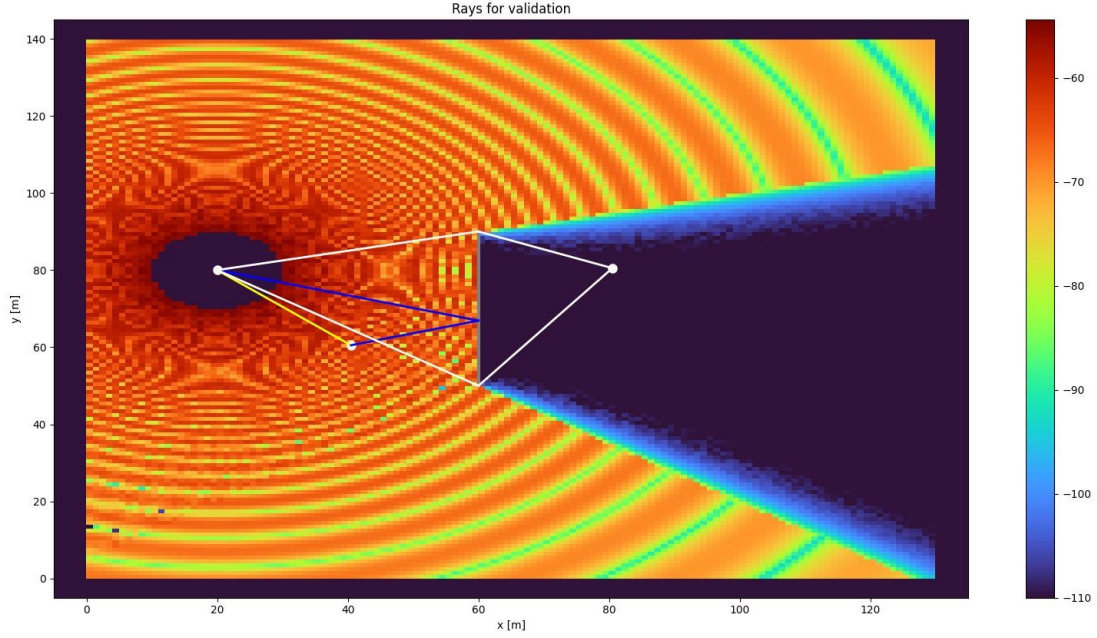


Figure 3.1: 2D heatmap of Power received in dBm and rays used for validation  
antenna RX 1 in (40.5,60.5) antenna RX 2 in (80.5,80.5)

	Simulation	Hand-calculation	Units
$V_{oc,LOS}$	$-5.34e-5 - j5.00e-4$	$-5.34e-5 - j4.99e-4$	V
$V_{oc,Ground}$	$1.24e-4 - j2.19e-4$	$1.2e-4 - j2.18e-4$	V
$V_{oc,Wall}$	$-2.35e-5 - j8.22e-5$	$-2.18e-5 - j7.64e-5$	V
$V_{oc,Diffraction}$	$1.56e-6 + j1.90e-7$	$1.55e-6 + j1.90 e-7$	V
$\Gamma_{Ground}$	-0.52	-0.51	/
$\Gamma_{Wall}$	-0.377	-0.35	/
$\ F(\nu)\ $	6.67e-3	6.67e-3	/
$\nu$	33.95	33.95	/
$arg\{F(\nu)\}$	-1811.68	-1811.68	rad
Prx,1	1.10e-9	1.08e-9	W
Prx,2	7.06e-15	7.06e-15	W

## 4. Results and Models

### 4.1 Results for the full 2D map

The simulation has been applied to a concrete case of antenna deployment, with a more complicated structure. Here, the value of the received power and other communication parameters were computed for the Grand Place of Brussels and its adjacent streets. A 2D map of the square was discretised into antennas placed at the center of square of  $1m^2$  and the results were displayed on 2D heatmaps.

Figures 4.1 to 4.4 show the received power at UE for different types of rays.

Fig 4.1: Considering only the LOS ray we observe a progressive decay of the received power that looks like the free space model.

Fig 4.2 : Once we add the ground reflected ray, we observe circular patterns which are due to the path length difference of those two rays, slowly varying with the distance in the far field.

Fig 4.3: When summing the wall reflected rays as well, we observe fast fading around the previous value, due to the uncorrelation of the phase of each component.

Fig 4.4: Finally, diffracted rays are orders of less powerful than other types of ray and do not cover much surface area (with sufficient power).

The combination of all rays tells us how much power is received at each antenna (see fig 4.5)

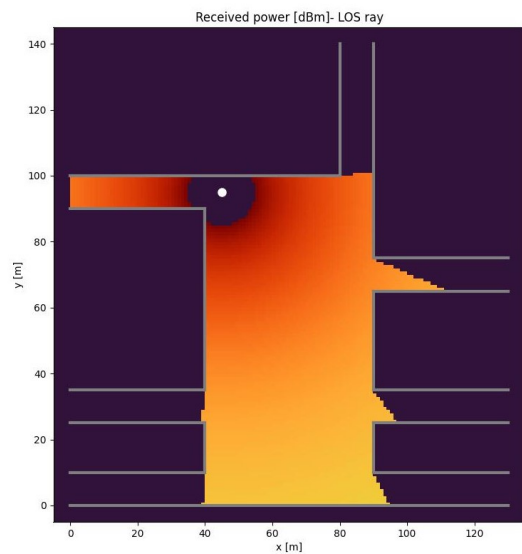


Figure 4.1: LOS ray

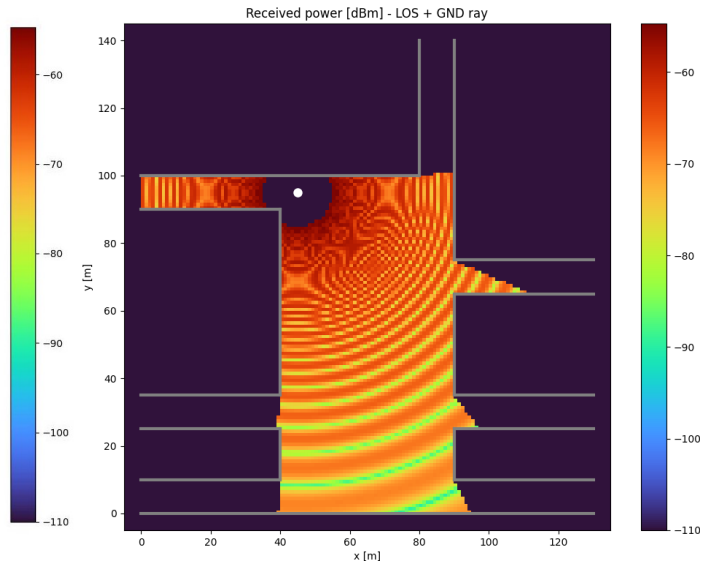


Figure 4.2: LOS + ground rays

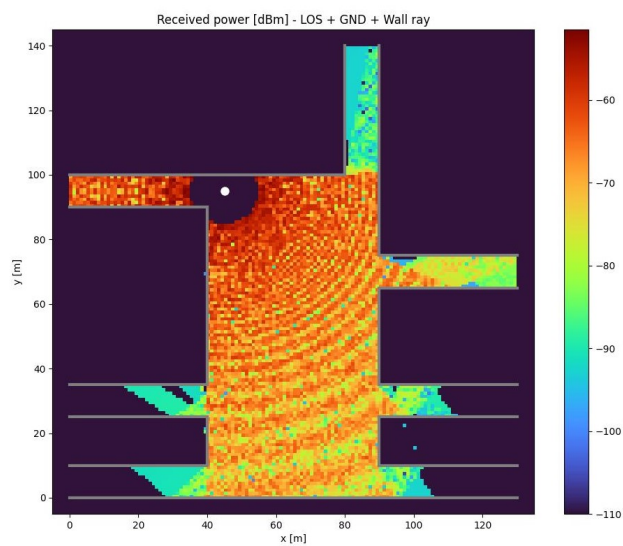


Figure 4.3: LOS + ground + Wall reflections

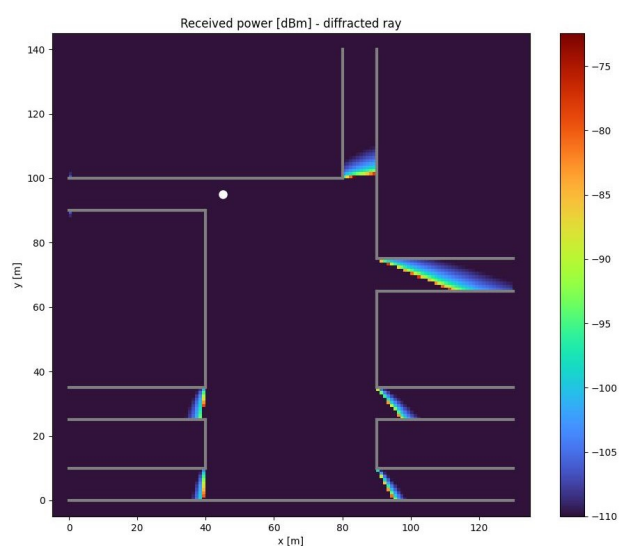


Figure 4.4: Diffracted ray

Received power from different rays combined

The SNR, on Fig 4.6, is computed as follow:

$$SNR[dB] = P_{RX}[dBW] - NoisePower[dBW] = P_{RX}[dBW] - F_{dB} - 10\log(kTB) \quad (4.1)$$

Where  $F_{dB}$  is the noise figure that characterise the noise added by the receiver electronics and  $-10\log(kTB)$ , the thermal noise( $T = 300K$ ,  $B = 200$  MHz).

The delay spread, on Fig 4.11, is the maximum delay between two incoming rays at UE. To compute it, we need to know the length of each ray and apply this equation, where  $d$  is the ray length and  $c$  the speed of light:

$$\sigma_\tau = \frac{\max_{i,j} |d_i - d_j|}{c} \quad (4.2)$$

The delay spread is bigger on the square than in the streets because the difference between the LOS ray length and the 2 reflection ray can be very big. Of course, the residual power of such long and twice reflected ray is very small and a more realistic computation of the delay spread, using the power delay profile, may result in a different result.

The Rice Factor, on Fig 4.12, gives the relative power of the LOS component compared to the mean power received from the other components:

$$K[dB] = 10\log\left(\frac{a_0^2}{\sum_{n=1}^N a_n^2}\right) \quad (4.3)$$

We can observe a diminution of the rice factor with the distance, which is correlated with the reduction of the LOS power seen in figure 4.1. The openings of the square causes the rice factor to increase as no reflection is possible there.

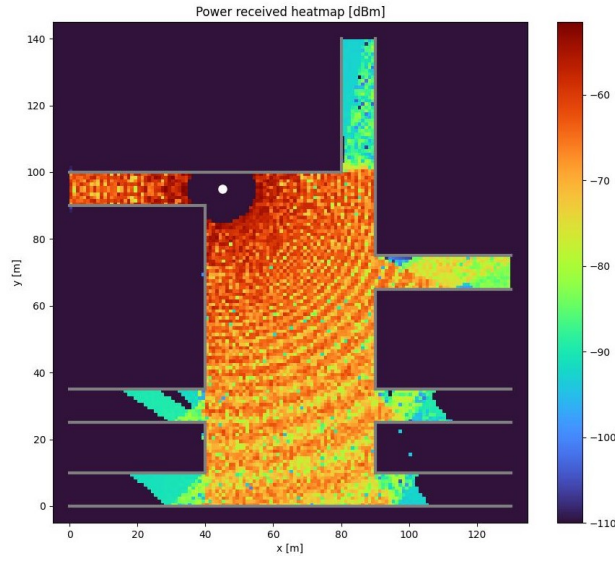


Figure 4.5: Power received [dBm]

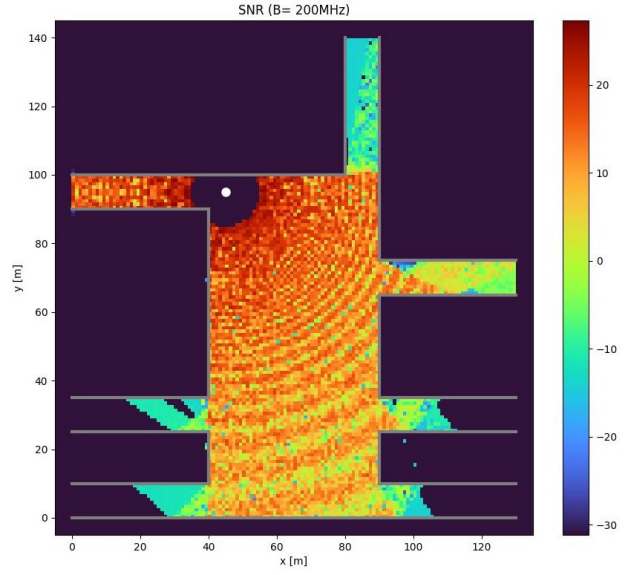


Figure 4.6: SNR [dB]

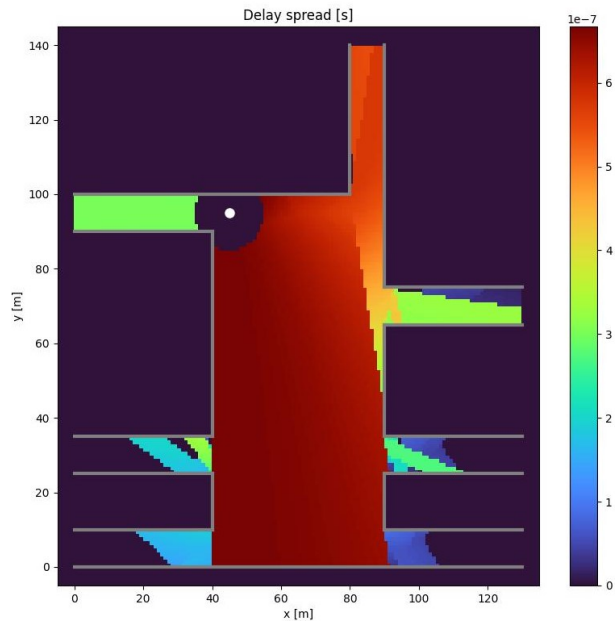


Figure 4.7: Delay spread[s]

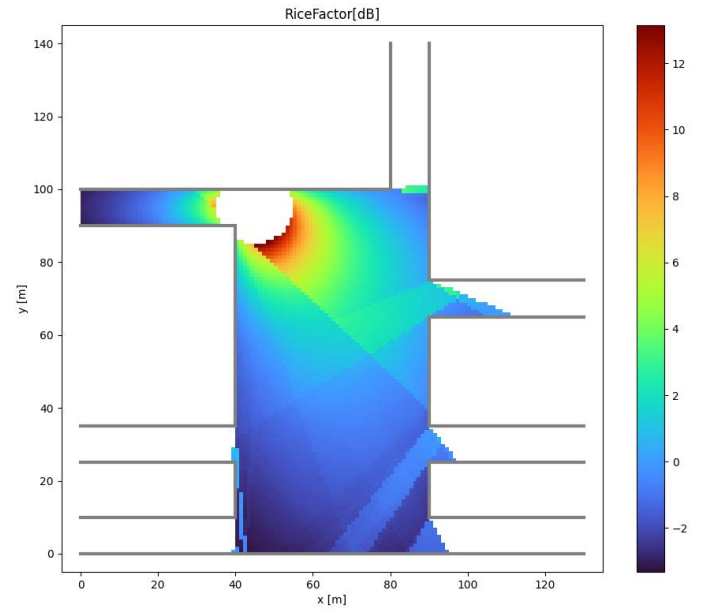


Figure 4.8: Rice factor[dB]



## 4.2 1D distribution from BS to eastern corner

Using the same method on a series of 500 receiver antennas positioned between the BS and the eastern corner (90, 0), the following 1D distributions were computed for each parameter.

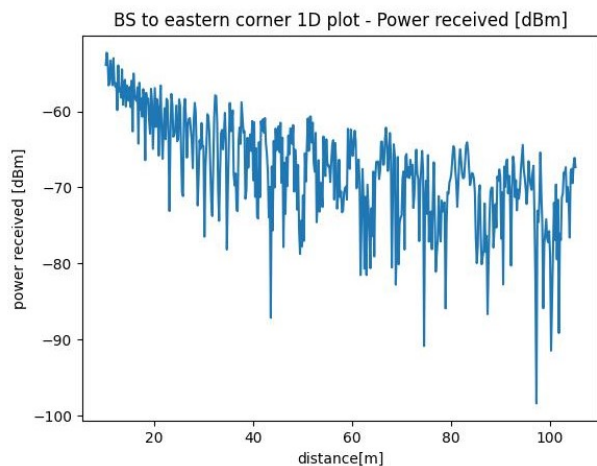


Figure 4.9: Power received [dBm]

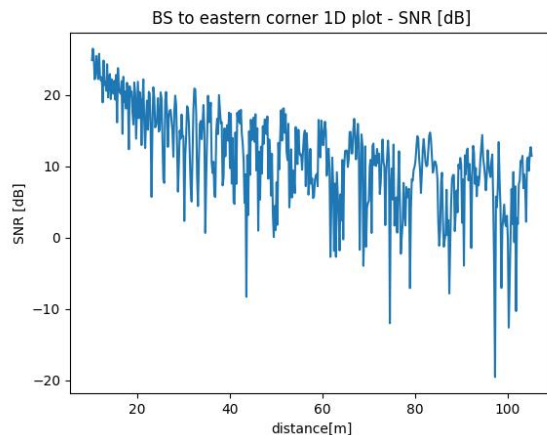


Figure 4.10: SNR [dB]

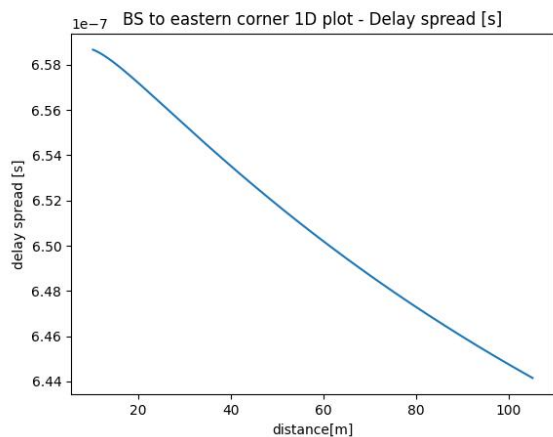


Figure 4.11: Delay spread[s]

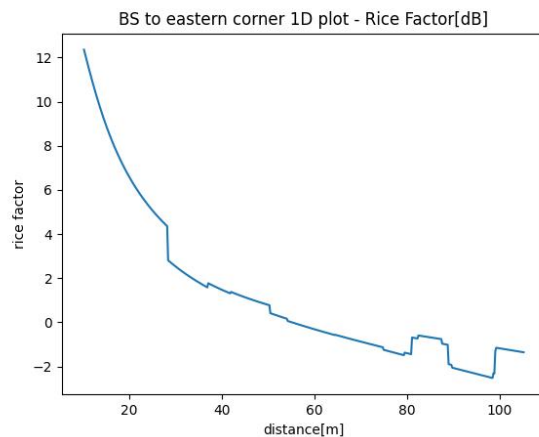


Figure 4.12: Rice factor[dB]

## 4.3 Model evaluation

From the 1D distribution of received power, one can build a model of propagation for the Grand Place and estimate the cell range based on this model.

### 4.3.1 Path loss model

The path loss  $L$  is defined as the ratio between the transmitted power  $P_{TX}$  and the averaged received power. In log scale, it is given by equation 4.4. Building a path loss model consists in finding the parameters for which equation 4.5 fits the calculated data at best. The path loss exponent "n" expresses how fast the averaged power received decreases with the distance from BS. And  $\langle P_{RX}(d_0) \rangle$  is the averaged power received at a distance  $d_0$ .

$$L[\text{ dB}] = P_{TX}[\text{dBm}] - \langle P_{RX} \rangle [\text{dBm}] \quad (4.4)$$

$$\langle P_{RX}(d) \rangle [\text{dBm}] = \langle P_{RX}(d_0) \rangle [\text{dBm}] - 10n \log \frac{d}{d_0} \quad (4.5)$$

"n" and  $\langle P_{RX}(d_0) \rangle$  are the coefficients of the 1st order approximation that fits the log-log graph of the power distribution. It has been drawn in orange of figure 4.13. In this model,  $n = 1.80$  and  $\langle P_{RX}(10m) \rangle = -55.2 \text{ dBm}$

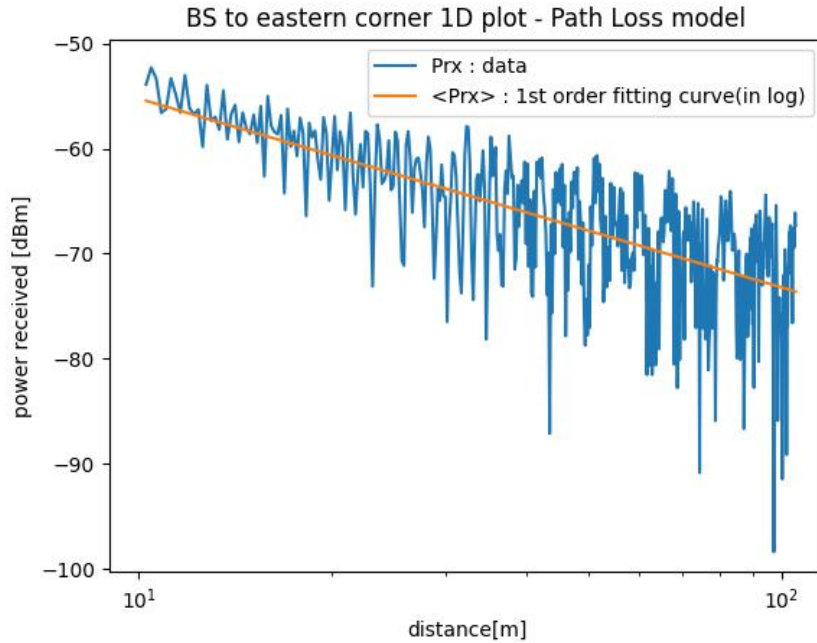


Figure 4.13: Path loss model fitting the received power

### 4.3.2 Fading Variability

As one can see on Fig4.13, the distribution vary a lot around the model, causing the received power to be below its average value half of the time. This is called fading and it will affect the probability of connection. The actual data can be seen as a random variable of mean value  $\langle P_{RX}(d) \rangle$  and of variance  $\sigma_L = 5.01$ . This variance can easily be found by computing the variance of  $P_{RX}(d) - \langle P_{RX}(d) \rangle$ . This has been plotted on figure 4.14

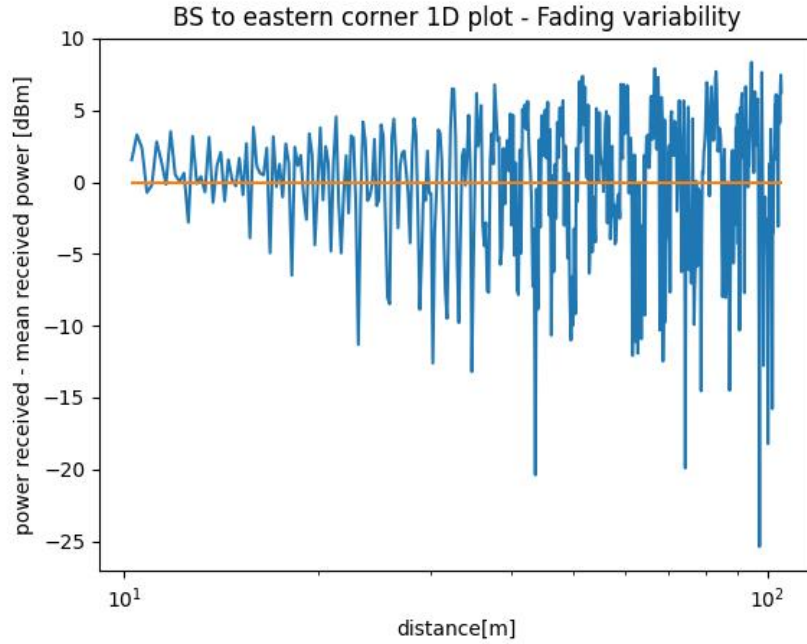


Figure 4.14: Fading variability around the fitting curve

### 4.3.3 Cell range

The cell range is the distance from the BS at which you can expect to have a certain probability of connection. At cell edge, the probability that the fading increases the path loss by at least  $\gamma$ dB is given by:

$$\Pr [L_{\sigma_L} > \gamma] = \frac{1}{2} \operatorname{erfc} \left( \frac{\gamma}{\sigma_L \sqrt{2}} \right) \quad (4.6)$$

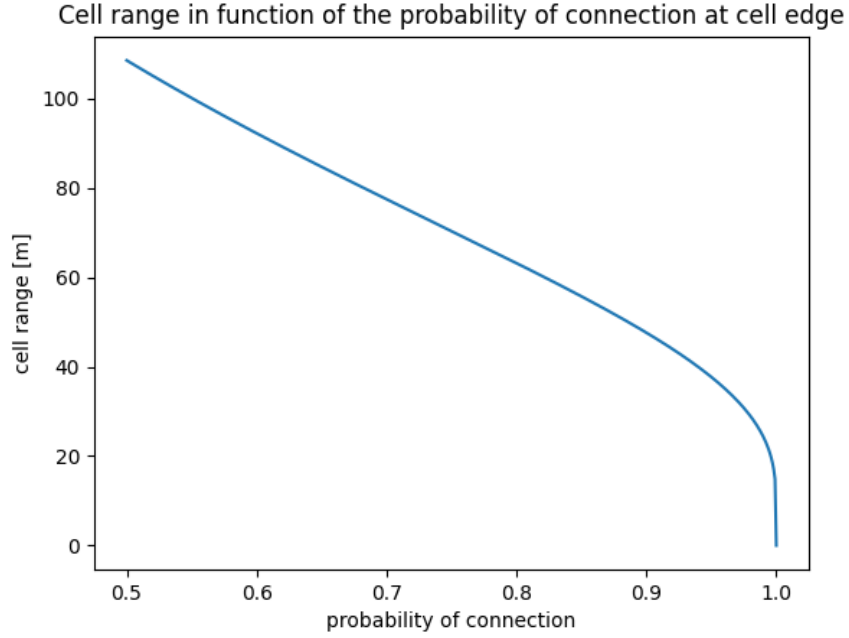


Figure 4.15: Cell range as a function of the probability of connection

This means that taking into account an extra fade margin of  $\gamma$ , we can have a probability of connection of  $1 - \Pr[L_{\sigma_L} > \gamma]$  at the distance where :

$$< P_{RX}(d) > [dBm] - \gamma = < P_{RX}(d_0) > [dBm] - 10n \log \frac{d}{d_0} - \gamma = ReceiverSensitivity[dBm] \quad (4.7)$$

The receiver sensitivity is given by :

$$ReceiverSensitivity[dBm] = TargetSNR[dB] + F_{dB} + 10 * \log\left(\frac{kTB}{1mW}\right) = -73.82dBm \quad (4.8)$$

This distance is the cell range for a certain probability of connection and has been plotted on figure 4.15.

## 4.4 Impulse responses

### 4.4.1 Center of the square

The rays reaching the center of the square in (65.5, 50.5) have been drawn on figure 4.16

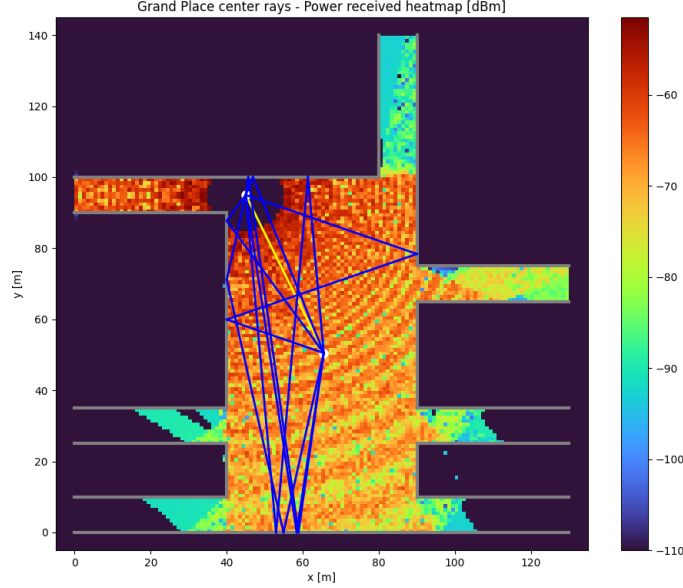


Figure 4.16: Rays reaching the center of the square

The physical impulse response of the channel is:

$$h(t, \tau) = \sum_{n=1}^N a_n(t) e^{j\phi_n(t)} e^{-j2\pi f_c \tau_n} \delta(\tau - \tau_n) = \sum_{n=1}^N \alpha_n(t) \delta(\tau - \tau_n) \quad (4.9)$$

In our case the channel is time invariant and the physical impulse response display on figure 4.17 shows nine impulses corresponding to the 9 rays. The first impulse is the strongest, the LOS component followed closely by the ground reflection. Then the other MPCs take up to  $0.7\mu s$  to arrive.

The tapped delay line impulse response considers that all waves arriving during a delay tap of  $\Delta\tau = 1/2B$  sum up at the receiver and cannot be discriminated. But also, this model consider the non narrow bandwidth(eq:4.11), one MPC can be represented in different taps,

causing leakage.

$$h_{TDL}(t, \tau) = \sum_{l=0}^L h_l(t) \delta(\tau - l\Delta\tau) \quad (4.10)$$

$$h_l(t) = \sum_{n=1}^N \alpha_n(t) \text{sinc}(2B(\tau_n - l\Delta\tau)) \quad (4.11)$$

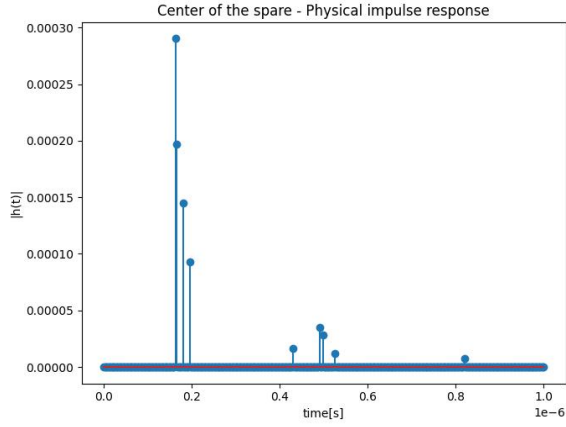


Figure 4.17: Physical impulse response

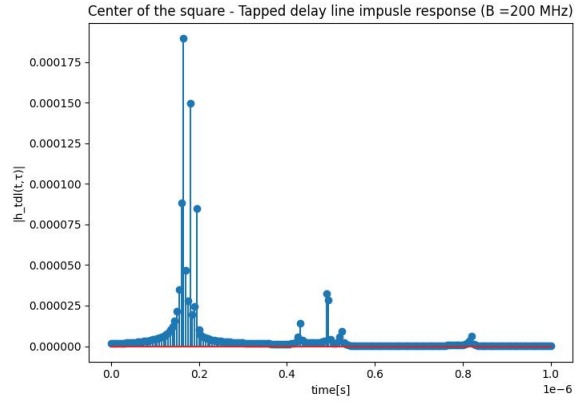


Figure 4.18: TDL impulse response (B = 200MHz)

#### 4.4.2 Eastern corner

The rays reaching the center of the square in(65.5, 50,5) have been drawn on figure 4.16

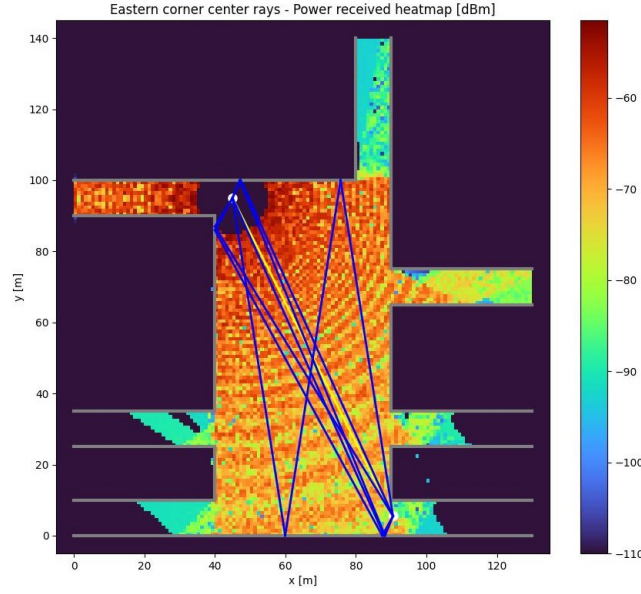


Figure 4.19: Rays reaching the eastern corner

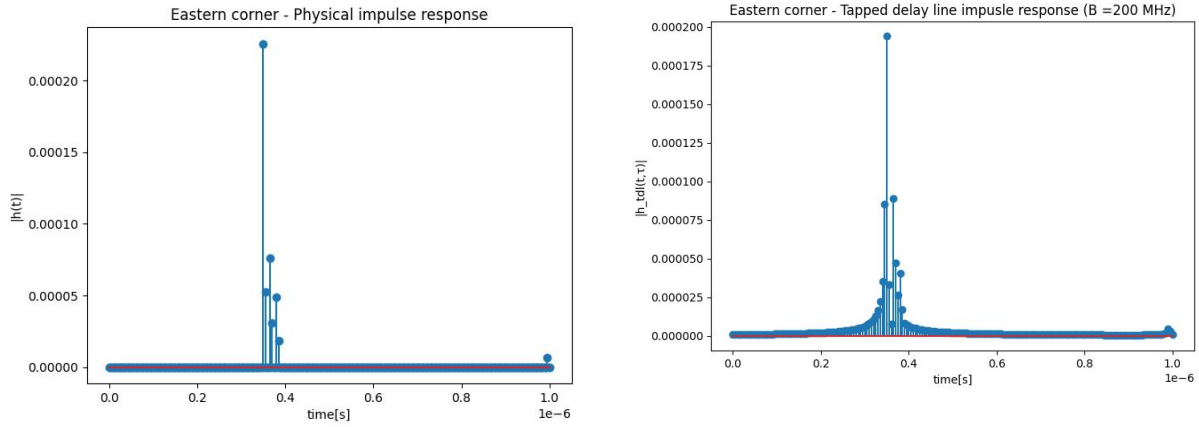


Figure 4.20: Physical impulse response

Figure 4.21: TDL impulse response ( $B = 200\text{MHz}$ )

The physical impulse response shows 7 impulses although there are more MPC because some of them have very close delays and sum up. The tapped delay line impulse response of such close MPC causes leakage and makes it impossible to discriminate the MPCs.

## 5. Further discussion

### 5.1 Propagation model for the rue de la Tête d'Or

A propagation model was also proposed for rue de la Tête d'Or which is the western street close to the BS. The street propagation is modeled out of a distribution of power over 100 meter using 1000 antennas, as it can be seen of Figure 5.1.

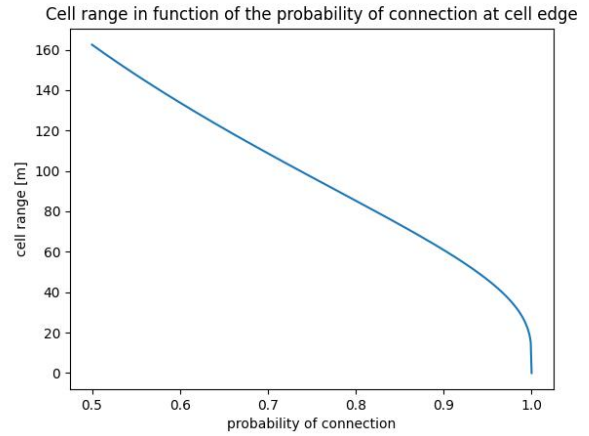
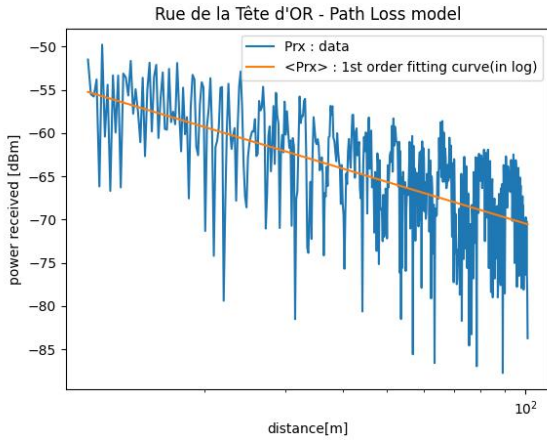


Figure 5.1: Power received distribution for rue de la Tête d'Or

Figure 5.2: Cell range for the rue de la Tête d'Or

$$n_{rue} = 1.29, < P_{RX,rue}(10m) > = -56.8 \text{ dBm and } var_{rue} = 5.18$$

$$n_{gp} = 1.80, < P_{RX,gp}(10m) > = -55.2 \text{ dBm and } var_{gp} = 5.01.$$

Both situation are sort of urban canyon geometries, although the Grand place has its walls more separated and is subject to shadowing as they are openings in the square and walls above and below. This type of geometry tends to guide the waveform and its energy in a specific direction, explaining the smaller path loss exponent in comparison to Friis model



(n=2). The street is even better at this than the square so that  $n_{rue} < n_{gp}$ . The same idea applies to the cell range for 90% of connection that has increased from 47m to 63m.

## 5.2 Reflectors and directivity manipulation

The problem I wanted to solve is that there are no public furniture on the Grand Place so that we could only place our antennas on the walls.

To prevent loss of power into the wall, metal sheets of 1 meter wide were added between the wall and the antenna, with a reflection coefficient of  $\Gamma_{perp} = -1$ . The effect is double edge, as one can see on figure 5.4. On one hand, the directivity of the antenna is stronger in some directions but lower in other. This is due to the LOS and reflector rays that are either constructive or destructive. On the other hand, the model parameters for the grand place are improved using the reflector at  $d = 5/4\lambda$  from an antenna against the western top wall:

$$n_{rue} = 2.08, < P_{RX,rue}(10m) > = -57.0 \text{ dBm and } var_{rue} = 4.9$$

$$n_{gp} = 1.53, < P_{RX,gp}(10m) > = -55.3 \text{ dBm and } var_{gp} = 3.6$$

Finally, this section will try to compute the distance between the reflector and antenna that maximise the directivity towards the streets.

### 5.2.1 Development of the directivity of the antenna + reflector

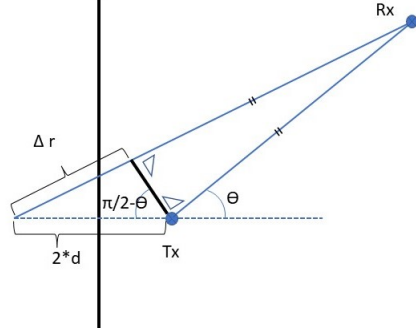


Figure 5.3: Geometry of the reflector with 2 rays

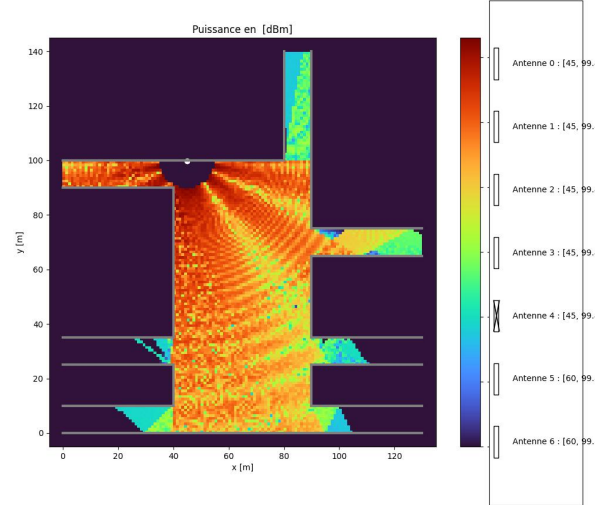


Figure 5.4: Power received[dBm],  $d = 5/4 \lambda$  at (45,100)

As we can see on Figure 5.3, when the UE is far from the BS, the isosceles triangular has 2 corners that tend to  $\pi/2$ . Using this approximation, we can compute the path length difference,  $\Delta r$ , between the LOS and reflected ray:

$$\sin\left(\frac{\pi}{2} - \theta\right) = \frac{\Delta r}{2d} \quad (5.1)$$

We also know that :

$$E_{LOS} + E_{REF} = \alpha_{LOS}(r)(1 - e^{-j\Delta r \frac{2\pi}{\lambda}}) \quad (5.2)$$

Which is maximum when:

$$\Delta r = \frac{(2n + 1)}{2} \lambda \quad (5.3)$$

Therefore, for the antenna of figure 5.4, with  $d = 5/4\lambda$ , constructive interferences are located at  $\theta = \{0^\circ, \pm 53.1^\circ, \pm 78.4^\circ\}$  which corresponds to our results. It also explains why the power dropped quickly in the rue de tête d'or,  $78^\circ$  is not enough to point the beam towards the end of the street.

It is interesting to notice that increasing  $d$ , we are increasing the number of lobes (see

Appendix for visuals B)

### 5.2.2 Directing the beam towards the streets

The same set of equations can be used to redirect the power at a certain angle. The angle between (65,0) and the street at (90,30) is  $\theta = 0.695rad$  so that with  $n=1$  and  $d = 0.97 \lambda$  we can point the beam in this direction. See results on figure 5.5.

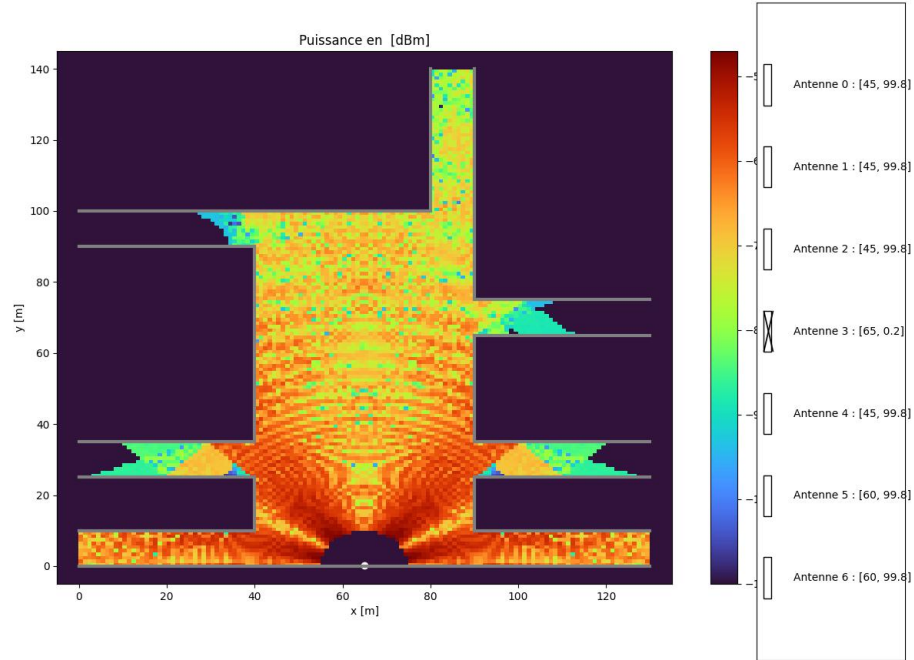


Figure 5.5: Power received,  $d = 0.97\lambda$

## 5.3 Optimisation using an interactive interface

To optimise the position of each antenna the user can use an interface to quickly remove or add antennas whose power heatmap have been saved. It allow the user to better understand the impact of adding antennas. The configuration proposed below (figure 5.6) is constituted of one antenna in (60, 100) ( $d = 3/4 \lambda$ ) and the one calculated before in (65,0) ( $d = 0.97 \lambda$ ) tend to minimize the number of regions with a received power below -73,8dBm, the receiver sensitivity.

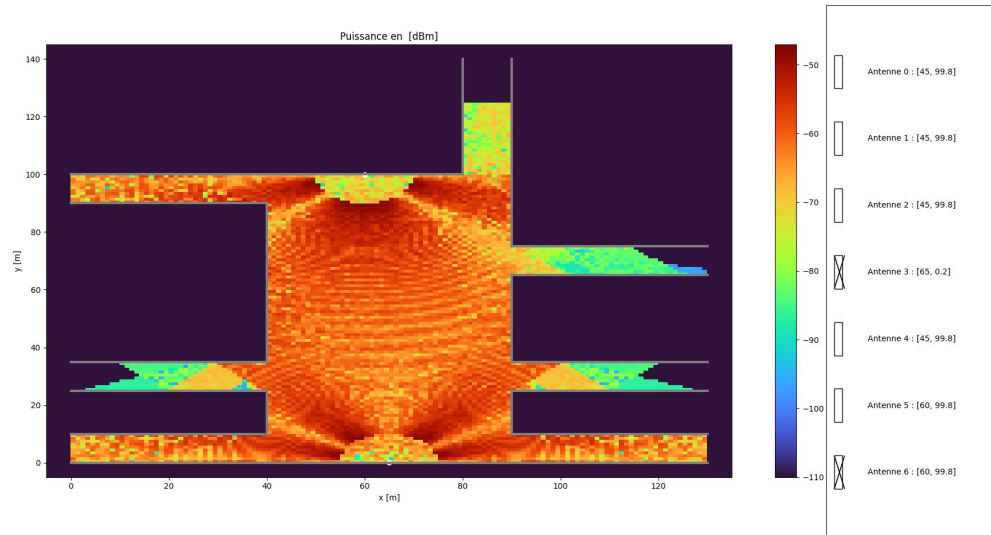


Figure 5.6: Proposed configuration

## 6. Conclusion

Finally, this project has lead to a working ray-tracing algorithm that is able to compute the power distribution over the Grand place and in its adjacent street. We have realised how complicated it may be to communicate in the street around the grand place, especially using only BS on the buildings. Using a sort of controlled beam forming by using a reflector behind the antenna, helped redirecting part of the power towards the grand place rather than the street. Also using this principles we were not only able to predict the angles at which there would be constructive interferences but also choose a distance between the reflector and the antenna that would point the beam towards a point of interest, the streets.

## A. TDL impulse responses

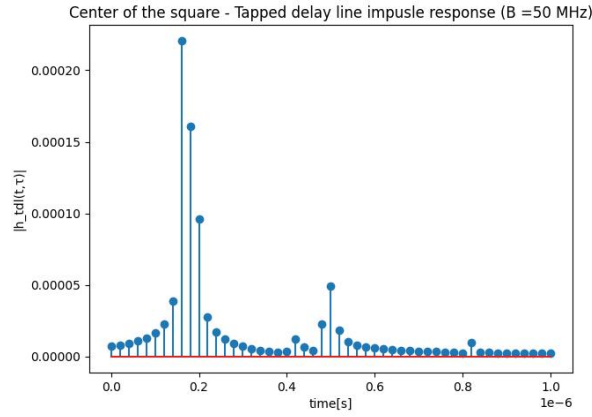


Figure A.1: TDL impulse response ( $B = 50$  MHz)

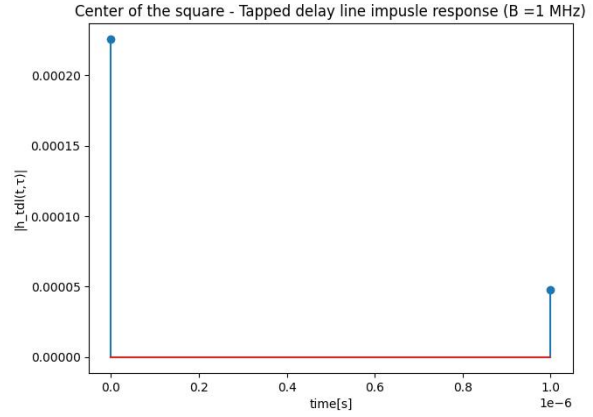


Figure A.2: TDL impulse response ( $B = 1$  MHz)

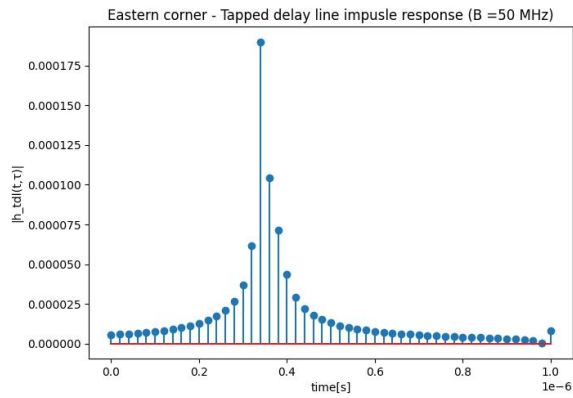


Figure A.3: TDL impulse response ( $B = 50$  MHz)

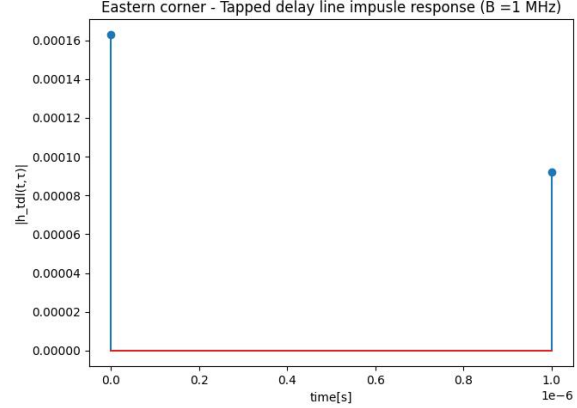


Figure A.4: TDL impulse response ( $B = 1$  MHz)

## B. Interferences obtained for different values of d

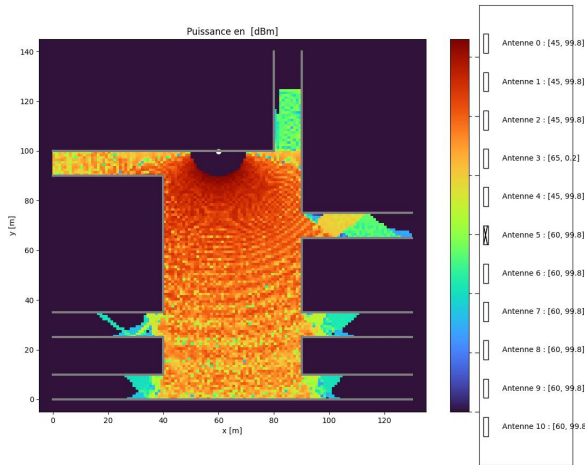


Figure B.1:  $d = 1/4 \lambda$

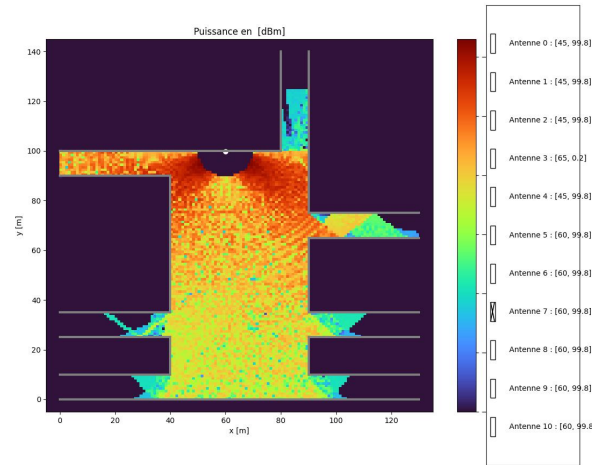


Figure B.2:  $d = 3/4 \lambda$

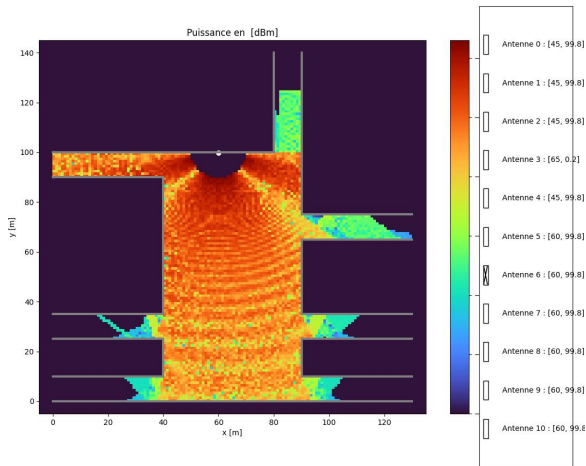


Figure B.3:  $d = 1/4 \lambda$

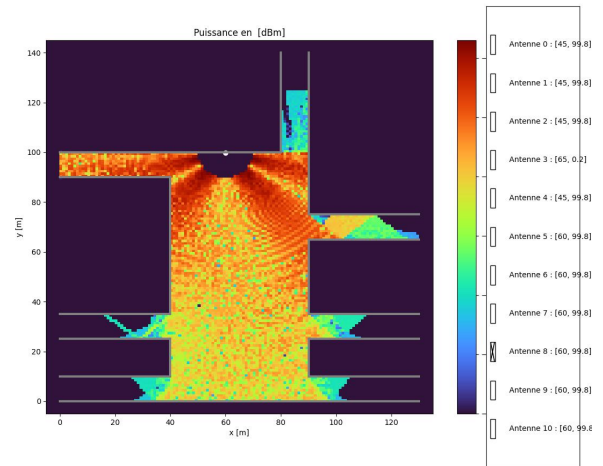


Figure B.4:  $d = 4/4 \lambda$

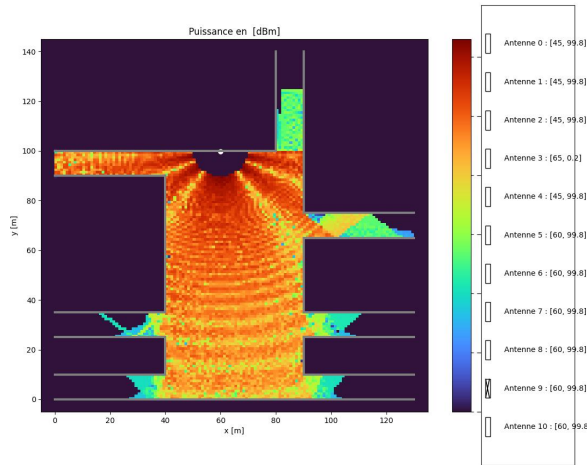


Figure B.5:  $d = 5/4 \lambda$

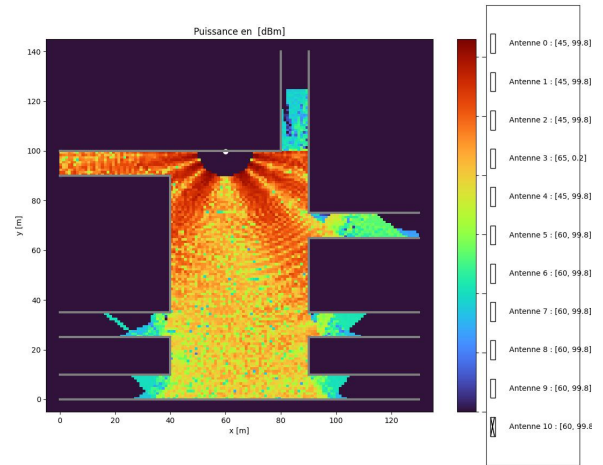


Figure B.6:  $d = 6/4 \lambda$